Surface & Coatings Technology 357 (2019) 36–47

Contents lists available at ScienceDirect

Surface & Coatings Technology

journal homepage: www.elsevier.com/locate/surfcoat

Physicochemical bisphosphonate immobilization on titanium dioxide thin films surface by UV radiation for bio-application

Erika S. Bronze-Uhle[a], Leonardo F.G. Dias[a], Luciana D. Trino[a], Adriana A. Matos[b], Rodrigo C. de Oliveira[b], Paulo N. Lisboa-Filho[a,*]

[a] UNESP - São Paulo State University School of Sciences, Department of Physics, Bauru, São Paulo, Brazil
[b] Department of Biological Sciences, Bauru School of Dentistry, University of São Paulo, Bauru, São Paulo, Brazil

ARTICLE INFO

Keywords:
Titanium
Titanium dioxide
Functionalization
Bisphosphonate
Alendronate
Risedronate and bone implant materials

ABSTRACT

Titanium and its alloys have been routinely used to replace bone and teeth. This success is mainly due to their remarkable clinical response, mechanical properties, chemical stability and appropriate biocompatibility associated to a titanium dioxide (TiO_2) layer. Chemically, the TiO_2 surface is mostly terminated by −OH groups. An increased amount of reactive −OH groups can be obtained by UV radiation treatment on TiO_2 surface, which can be readily functionalized with bifunctional organic molecules. Among the several types of organic molecules available for reaction with −OH groups, bisphosphonates (BP) have been associated with a positive effect on new bone formation. In this way, the present contribution aims at giving an overview study from the physicochemical properties of two distinct BP (alendronate and risedronate), immobilized on the titanium surface containing hydroxylated TiO_2 film by UV radiation. Surface properties such as contact angle, surface free energy and topography/roughness were evaluated. In addition, biocompatibility and mineralization tests performed with osteoblastic-like cells are presented to evaluate the potential of these functional materials to be applied in the dentistry and orthopedics fields. The results suggest that the UV treatment increased the surface wettability and allowed an oriented immobilization of BP. In addition, the BP functionalized surfaces exhibited high viability and mineralization of pre-osteoblast cells. Therefore, these compounds emerge as a potential treatment on implants surfaces.

1. Introduction

Titanium and its alloys are extensively used as biomaterials for implants in medicine and dentistry due to their excellent mechanical properties, chemical stability, biocompatibility and applied clinical response [1–6]. The physicochemical properties of titanium that confer good biological performance are closely related to its surface characteristics such as morphology, chemistry and wettability. Titanium surface topographical modifications have been studied combining micro e nanoscale features to mimic the characteristic of natural bone, as osteointegration [7–9].

It is well known that metallic titanium has an amorphous native titanium dioxide (TiO_2) thin layer (5–6 nm) on its surface, which is associated with the improved biocompatibility properties of titanium when compared to other metals [10]. However, Maitz et al. [11] evaluated that the native oxide layer was generally less hemocompatible compared to a thicker and more homogeneous layer of TiO_2. In addition, studies have shown that a thicker and homogeneous TiO_2 coating (100 nm) significantly increased the long-term bio-corrosion titanium resistance, showing a similar cellular response [10]. Therefore, the TiO_2 crystallinity, hydrophilicity, and surface chemistry are extremely important in the bone integration process [12,13]. Furthermore, the deposition of TiO_2 in the nanometric phase can result in better adhesion and proliferation of osteoblasts. In this way, the titanium surface modification with a nanometric, crystalline and homogeneous TiO_2 film can be accomplished through different methods of deposition, such as spin coating technique [14].

Nanostructured titanium dioxide presents high dielectric constant, high hardness and chemical stability and, due to these characteristics, has been used as surface modifier in different applications, such as the use of semiconductor nanomaterials, anticancer drug transporters and biomedical implants [15–18]. In biomedical applications, recent research has emphasized that the optimization of implant bone anchorage is mainly focused on modified and hydrophilic TiO_2 surfaces during early stages of osteointegration [19]. In addition, several surface TiO_2 modification procedures have been studied in order to induce chemical

* Corresponding author.
E-mail address: paulo.lisboa@unesp.br (P.N. Lisboa-Filho).

https://doi.org/10.1016/j.surfcoat.2018.09.038
Received 3 July 2018; Received in revised form 13 September 2018; Accepted 15 September 2018
Available online 25 September 2018

surface functionalities to adjust the physical and chemical properties of the surface with adhesion, biocompatibility and cellular proliferation.

Surface manipulation involves a large number of experimental procedures, in terms of surface modification and interfaces, for the study of the interactions between bulk and surface modifier. This can improve the corrosion resistance the material and increase oxide bioactivity, presenting promising results in the interaction with the tissue, since the biocompatibility is determined by chemical processes that occur in the interface between the prosthesis and the living tissue [19,20]. Studies have shown that monolayers formation on the titanium surface can change the topography and surface chemistry generating a material with new physical and/or biochemical properties by changes in surface energy, wettability and topography of biomaterial [21]. This could provide promising functional materials with molecular structure controlled allowing cell adhesion and proliferation [8,22,23].

Chemically, the TiO_2 surface is mainly terminated by hydroxyl groups, which can dissociate into solution. This can generate positive, negative or neutral charges, depending on the pH. The surface −OH groups and the charges formed by the dissociation play an important role in the connection with polymers, proteins and immobilization of organic molecules [24]. The amount of −OH groups on the TiO_2 surface influences the catalytic photo-activity and the hydrophilicity properties of the film [25]. It has been reported that the TiO_2 film hydrophilicity and surface energy increase through the combination of photo-activation mechanisms and structural changes in the surface by the enhancement of −OH groups [26–29]. Studies have shown that ultraviolet (UV) radiation incident on TiO_2 film alters the physical-chemical properties of the surface. UV radiation removes hydrocarbons and/or leads to the formation of reactive hydroxyl radicals generating highly hydrophilic surface without altering the topography [30–32].

An improvement in wettability/hydrophilicity is generated by the photoinduced cleavage of Ti−O bonds by increasing −OH groups on the surface, which favors the adhesion and proliferation of osteoblasts [33–35].

The presence of hydroxyl groups on the TiO_2 surface allows the covalent bonds formation with bifunctional bioactive organic compounds through condensation reactions, forming self-assembled monolayers (SAMs) on the oxide surface [21]. The surface modification by covalent bonds provides the possibility of immobilization and specific orientation of molecules. These bifunctional molecules can alter the chemical and morphological characteristics of the surface, included wettability and nanotopography modifying the interface properties between the cells and the implant, as well osteoblastic cell response. In general, a roughness and hydrophilic surface could stimulate proliferation and differentiation of osteoblasts during the osteointegration process [8,36–40].

The formation of SAMs can occur through specific adsorption conditions and reaction between one of the organic molecule functional groups with the hydroxyls from the substrate. The other terminal group is free to bind with proteins, cells, or even induce the formation of calcium phosphate crystals [40–43], making the biological response faster and more specific [43]. However, depending on the bifunctional compound used, some problems can occur, as surface hydrolysis and the formation of a non-homogeneous monolayer. Among the bioactive and bifunctional molecules, the bisphosphonates (BPs) emerge as an alternative with homogenous functionalization of TiO_2 surfaces since they are not susceptible to cell medium hydrolysis.

Bisphosphonates are compounds commonly used in treatments associated with metabolic bone disorders, in particular Paget's disease, malignant hypercalcemia, osteoporosis and osteopenia [44–46]. In addition, some studies also indicated that BPs may modulate inflammatory bone loss around total hip replacements induced by wear debris [44]. Bisphosphonates are stable synthetic drugs analogous to pyrophosphates, naturally occurring in the body. Pyrophosphates act on the physiological regulation of calcification and bone resorption [47,48]. Thus, synthetic drugs, like pyrophosphates, act as potent inhibitors of bone resorption and inhibit in vivo calcification of soft tissues, binding strongly to the bone mineral, hydroxyapatite, inhibiting its crystallization and dissolution [49,50].

Chemically, the BPs differ from the pyrophosphates, on which the central oxygen atom of the P−O−P bond is replaced by a central carbon atom P−C−P, which increases the solubility of these compounds in water and gives the compound greater resistance to chemical and enzymatic hydrolysis. The chemical structure of the BPs presents two phosphate groups ($-PO_3$) covalently linked to a central carbon and two chains, generically named as R1 and R2. The central P−C−P binding is responsible for the strong affinity of the drugs with hydroxyapatite. During interaction with hydroxyapatite, bisphosphonate becomes a highly charged acidic structure capable of chelating cationic ions, such as calcium, facilitating the inhibitory effects on bone metabolism in vitro and in vivo [48–50]. Both phosphate groups are required, and modifications in one or both R1 and R2 groups may significantly alter bone mineral affinity [51]. These groups act by different mechanisms affecting the intracellular processes essential for the cytoskeleton organization [52–54].

The strategies of BPs implant surfaces immobilization have been demonstrated to be efficient in osteoporosis patients during implant fixation [55], as well as in the control of biofilm formation at the implant-bone tissue interface [56]. The action mechanisms of BPs on the implants surface are not yet fully understood. However, it is known that BPs act to inhibit the proliferation of osteoclasts inhibiting bone resorption. Thus, the development of strategies for the immobilization of bisphosphonates on the TiO_2 surface may reduce possible adverse effects on the healthy tissue angiogenesis around the implant [57].

The present contribution aims giving an overview study from the physicochemical properties of two distinct bisphosphonates, alendronate and risedronate, immobilized on the titanium metal surface containing hydroxylated TiO_2 film. Surface properties such as contact angle, surface free energy and topography/roughness will be evaluated. In addition, biocompatibility and mineralization tests performed with osteoblastic-like cells are presented in order to evaluate the potential of these functional materials to be applied in the dentistry and orthopedics fields.

2. Materials and methods

2.1. Materials

Titanium samples were prepared from commercial pure titanium grade 4 (Ti cp4) discs, diameter 12.7 mm and thickness 3 mm, obtained from Acnis (Brazil). All others reagents were analytical grade and purchased from Sigma-Aldrich. All chemicals were used without any further purification. All aqueous solutions were prepared with a Millipore Milli-Q system.

2.2. TiO_2 synthesis solutions

The TiO_2 solution was prepared was prepared according to the protocol developed by Trino, L.D [58].

2.3. Preparation and modification of titanium substrates

The Ti cp4 discs were sandblasted in an Arotec polisher (Aropol-2v model) for 2 min using sandpapers granulometry of 320, 400, 600 and 800, obtaining substrates standardized with Ra value of ~194.91 nm ± 6.95 nm. Ti cp4 discs were cleaned with ultrapure water, isopropyl alcohol and again with ultrapure water for 10 min each, in an ultrasonic cleaner. Subsequently, the substrates were chemically cleaned in a highly acidic piranha solution mixture of 7:3 (v/v) 98% H_2SO_4 and 30% H_2O_2) for 2 h. Piranha solutions does react with the titanium, removing organic impurities and forms a more hydroxylated and hydrophilic surface [58,59]. After that the substrates were

rinsed in an ultrasonic cleaner with the same procedure related before for immediately oxide deposition.

The TiO_2 deposition was performed by spin coating technique (2000 rpm per 60 s) using a Headway Research INC (model PWM32-PS-R720) equipment. Over the metallic surface substrate three drops of TiO_2 solution were added. They were then placed in a hot plate at 40 °C for 5 min and the spin process deposition was repeated three times for each sample. After that, the samples coated with TiO_2 were annealed at 850 °C for 2 h in a heating rate of 1 °C min^{-1} in order to obtain a rutile crystalline polymorphic phase [58].

2.4. Surface hydroxylation

Thin films of TiO_2 were exposed to type C ultraviolet radiation using a commercially available photo device with 8 W (256 nm) UV-light source. Samples were illuminated at intervals of 10 to 105 min and contact angle measurements were performed immediately after exposure. After UV exposition the substrates, denominated TiO_2 (UV), were functionalized.

2.5. Preparation of SAMs

Alendronate and risedronate aqueous solutions were prepared at a concentration of 1 mg/mL. The TiO_2 substrates hydroxylated [TiO_2(UV)] and not UV-treated were immersed in the solutions containing the respective bisphosphonates at room temperature for 18 h. Afterwards, the samples were rinsed in water 3 times for 1 min to remove the physiosorbed alendronate or risedronate molecules. After the functionalization the samples were kept in vacuum at room temperature until further use. The samples were denominated TiO_2(UV)-Ale, TiO_2-Ale, TiO_2(UV)-Ris and TiO_2-Ris, for UV substrates treated and functionalized with alendronate, substrates without UV treatment and functionalized with alendronate, substrates UV treated and functionalized with risedronate and substrates without UV treatment and functionalized with risedronate, respectively.

2.6. Surface characterization

The crystalline phases of the TiO_2 deposited films were evaluated by a diffractometer system (XRD, D/MAX-2100/PC, Rigaku) using CuKα radiation within (k = 1.54056 Å) coupled to a nickel filter, in order to eliminate the CuKβ radiation. The samples were scanned from 20° to 45°, with regular step of 0.02 min^{-1} and scan speed of 2 min^{-1}, at 40 kV/20 mA. In order to determine the crystal structure, results were compared with PCPDF 65–3411, 44–1294 and 76–1949 cards for Ti and TiO_2, respectively.

Surface chemical composition was analyzed using X-ray photoelectron spectroscopy (XPS, Scienta Omicron ESCA), equipped with an EA125, Xm1000 monochromator and Al Kα X-ray source (1486.7 eV). Survey scans were completed at each region, followed by high resolution scans for C1s, O1s, P2p, and N1 s. Scans were aligned to the binding energy of the Ti 2p3/2 peak at 458.8 eV. Curve fitting was performed using the CasaXPS software. Peak identification was done to obtain a consistent fit for all the potentials investigated [60].

Contact angle and surface energy measurements were conducted in a goniometer (Ramé-Hart 100–00, Succassuna, NJ), by the sessile drop technique, using deionized water (polar substance), and diiodomethane (non-polar substance) as the probing liquids. The liquid was dropped automatically by a computer-controlled system and an image processing program determines the profile of this drop and then calculates the contact angle. The contact angle was measured 3 times with the same sample, on different positions, in an ambient air, and the average value was used. The results are expressed as a mean ± standard deviation for each experiment. The program also allows the surface energy of the material to be determined by harmonic and geometric methods, according to the Owens method [61], and energy magnitude was estimated by the sum of the dispersive component and the polar component generated by the liquids in contact with the substrate surface [62]. All measurements were carried out at room temperature and three spots were analyzed on each sample.

Surface topography and surface roughness measurements were evaluated using atomic force microscopy (AFM, Park System XE7, Santa Clara-USA) in non-contact mode. Analysis was conducted using a silicon cantilever (PPP-NCHR, Park Systems Corporate) having a constant force of 42.0 N/m and frequency of 330 Hz. The substrates were scanned in air under room temperature conditions. The images were taken using a scan rate in the range of 0.8 Hz, a peak force set point of 9.0 V, and a scan size performed over a 2.0 μm × 2.0 μm.

2.7. In vitro biocompatibility

2.7.1. Cell culture

Mouse preosteoblast MC3T3-E1 (subclone 14) cells (ATCC-*American Type Culture Collection*) were cultured in α-MEM (Minimum Essential Medium α, (Gibco, Carlsbad, CA) supplemented with 10% FBS (Fetal Bovine Serum, Gibco), 1% of 10.000 U penicillin-10 mg/mL streptomycin (Sigma-Aldrich) and kept at 37 °C in humidified atmosphere with 5% CO_2. After reaching the subconfluency the cells were subcultured using the enzyme trypsin (0.25% trypsin, 1 mM EDTA - Sigma-Aldrich), responsible for dissociating the cells from the culture flask, maintained for 5 min in the CO_2 incubator at 37 °C, then the enzyme was inactivated with α-MEM 10% FBS. Cells were centrifuged at 1200 rpm, 5 min at 4 °C. The supernatant was discarded, and the cells were diluted in a new α-MEM 10% FBS medium. Prior to cell platting, titanium samples (Ticp4, TiO_2(UV), TiO_2(UV)-Ale and TiO_2(UV)-Ris) were maintained for 30 min in ultraviolet light to reduce the risk of contamination [63].

2.7.2. MTT reduction assay

For the MTT reduction assay, 0.050 mL medium (αMEM + 10% FBS + 1% antibiotic) containing 2×10^4 cells was carefully added to the surface of each substrate to prevent cell adhesion in 24-well plates. After incubation for 4 h, at 37 °C in a humidified atmosphere with 5% CO_2, 1.0 mL of medium was then carefully added into each well. The assay was performed at 24, 48 and 72 h. In each experimental period, the wells were washed with phosphate buffered saline solution (PBS 1×), then the cells were incubated in a sterile MTT solution (0.5 mg/mL) for 4 h at 37 °C in a humidified atmosphere with 5% CO_2. The solution was removed and the intracellularly reduced insoluble pigment was extracted with DMSO (dimethylsulfoxide-Synth) at room temperature for 30 min. The experiment was in triplicate and tissue culture plastic was use as control. The extracted contents (n = 3/time point) were transferred to another 96-well plate to allow reading by absorbance at 550 nm (Synergy™ Mx Monochromator-Based Multi-Mode Microplate Reader, BioTek Instruments Inc.) [63–65].

2.7.3. Cellular morphology

The morphology and adhesion alteration of the preosteoblastic cells, on the titanium derivatives surfaces (Ti, TiO_2(UV), TiO_2(UV)-Ale, and TiO_2(UV)-Ris, were observed using a scanning electron microscope (EVO LS15, ZEISS, Oberkochen, Germany). For cell culture, MC3T3-E1 cells were incubated for 48 h (same MTT procedure), followed by removal of the medium and washing with PBS. The specimens were fixed in 2.5% glutaraldehyde and 1% osmium tetroxide for 2 h, and then washed with water. After this, the substrates were sequentially dehydrated using ethanol gradient solutions (50, 60, 70, 80, 90, and 100%) for 10 min each, followed by drying [66]. The specimens were coated with gold under Argon gas using a plasma sputtering system and then imaged at ×1000 magnification was taken.

2.7.4. Extracellular matrix mineralization

Quantification and detection of the amount of mineralized calcium

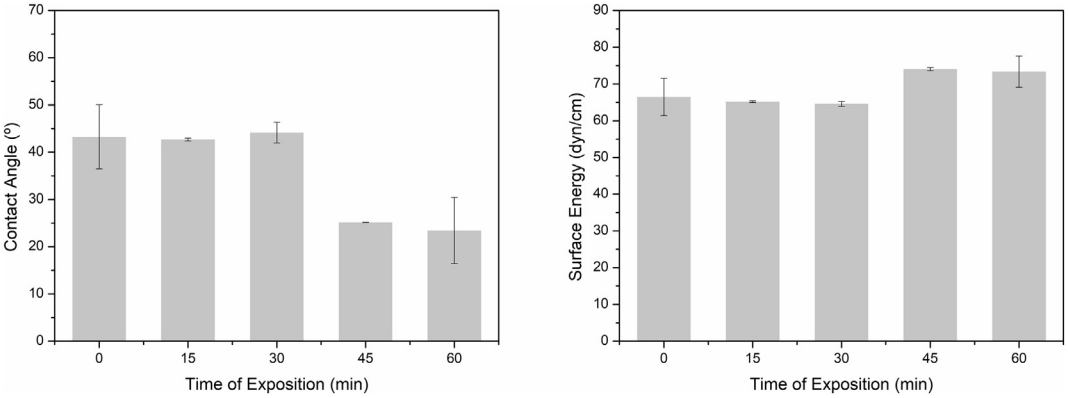

Fig. 1. Contact angle (a) and surface energy (b) measurements of TiO_2 substrates as a function of UV exposition time.

deposited in the extracellular matrix were performed by alizarin red staining. For the alizarin red assay, 0.050 mL of medium containing 5×10^4 cells/well (cultured as described above) were platted on the surface of substrates in 24-well plates, and 1.00 mL of medium was then added after 4 h of incubation. The assay was realized in 4 replicates, on plastic and differently Ti surfaces, for a period of 14 days. After this, the cells were rinsed with PBS three times and then fixed in 70% ethanol (0.70 mL) for 1 h at 4 °C. The cells were stained with 0.70 mL of Alizarin Red in ultrapure water for 10 min at room temperature. Then the cells were rinsed with ultrapure water until color disappeared and images were taken [67–69].

2.7.5. Statistical analysis

Statistical analysis of the cell assays were performed in the Graph Pad Prism 5 software (GraphPad Prism, GraphPad Software Inc., San Diego, California, USA) by selecting the one-way ANOVA statistical test complemented by the Tukey test, with the level of statistical significance set at $p < 0.05$.

3. Results and discussion

The obtained TiO_2 films deposited by spin coating technique over the Ti cp4 surface present nanometric scale, as reported elsewhere [58]. The XRD analysis indicated that the TiO_2 films show a characteristic rutile pattern phase according to PCPDF 65–191. Due to the high sintering temperature used to obtain the rutile phase, TiO_2 films presented particles size around 75 (± 6.4) nm and thickness of approximately 500 nm, determined by scanning electron microscopy according to previously published data [58].

The hydroxylation of the TiO_2 films surface was carried out in order to promote an improvement in the adsorption of biomolecules and consequently in the process of osseointegration, by modifying the TiO_2 hydrophilicity and wettability.

Hydrophilicity and wettability are intrinsically related surface components, represented by the surface energy of the material and the contact angle. The wettability of a surface depends on the thermodynamic equilibrium between solid, liquid and vapor interfaces. The magnitude of the surface energy is associated with the polar and dispersive components generated by the polar and apolar liquids in contact with the substrate, based on the contact angle measurements. Therefore, surface free energy and contact angle are directly associated with the surface chemical and topographic composition [32,35,39,67–71]. Some studies report the strong influence of hydrophilicity and/or hydrophobicity on the cell adhesion process, and a higher cell adhesion and proliferation was reported on surfaces with moderate hydrophilicity, having a water contact angle in the range of 60°–90° [37,72–74]. Interestingly, Vasilescu et al. reported that higher levels of cell attachment can be obtained on hydrophilic surfaces with contact angle in the range of 20°–40°. [75]. Others correlate the spreading and greater fibroblasts propagation with free surface energy higher than 45 (mN/m) [74]. Aita et al. [76] reported that, in vivo tests, the UV titanium surfaces treatment increase the hydrophilicity of the material by promoting the formation of new bone at the implant bone interface. However, there is no consensus about the ideal degree of hydrophilicity for cell adhesion, since it is highly dependent on topography and surface chemistry. An assessment of both factors is that will provide a better cellular response [72,77,78].

A qualitative confirmation that the surface was chemically modified can be obtained through contact angle measurements. The property related to the number of electrons on the surface and consequently correlated with the surface free energy. In addition, the contact angle represents a quantitative measure of the wettability process. In general, the higher the surface energy the greater the wettability and the better the adhesion between the material surface and the physiological media components [37,79,80].

High hydrophilic surfaces produce very low contact angles, converging 0° in to metallic or clean metal oxide surfaces. Small contact angles (< 90°) correspond to high wettability of the surface, while large contact angles (> 90°) correspond to low wettability [81]. The wettability and hydrophilicity of TiO_2 surfaces can be adapted from 0° to 170° by modification with UV irradiation and/or functionalization with organic compounds [82]. In general, the higher the wettability the greater the surface free energy and the better the adhesion between the material surface and the physiological media components [80–82].

To activate surface hydroxyl formation, TiO_2 films were exposed to ultraviolet type C radiation using an 8 W (256 nm) lamp [83]. In the process of UV irradiation, photons excite the surface of TiO_2 generating vacancies (□) of oxygen. The electron from the surface interact rapidly with adsorbed oxygen and/or water molecules filling the generated vacancies by oxygen, forming −OH groups on the surface [84–88] altering the hydrophilicity and surface energy.

The contact angle and surface energy values obtained for the TiO_2 film ($n = 3$), after different exposure times in the UV light lamp, are summarized in Fig. 1a and b.

The initial values of the contact angle and surface energy were 43.2° and 66.40 dyn/cm. After UV exposition it is observed that the lower contact angle value occurs at 45 min of exposure (23.9°) when compared to the samples without UV treatment (43.2°). In addition, it is important to mention that surface energy value changed, increasing from 66.4 dyn/cm to 72.4 dyn/cm. The differences of the contact angle and surface energy initial values indicated a highly hydrophilic state produced by UV irradiation after 45 min time. Although they have contact angle values that decreased with exposure time in UV light exposure, the surface energy for the substrates are very similar, as can be seen in Fig. 1b. Polar components are expected to attract water dipoles and minimize contact angle. Thus, the increase of the polar components, by the formation of hydroxyl groups on the surface, would lead to an increase in the total free energy of the surface as observed in

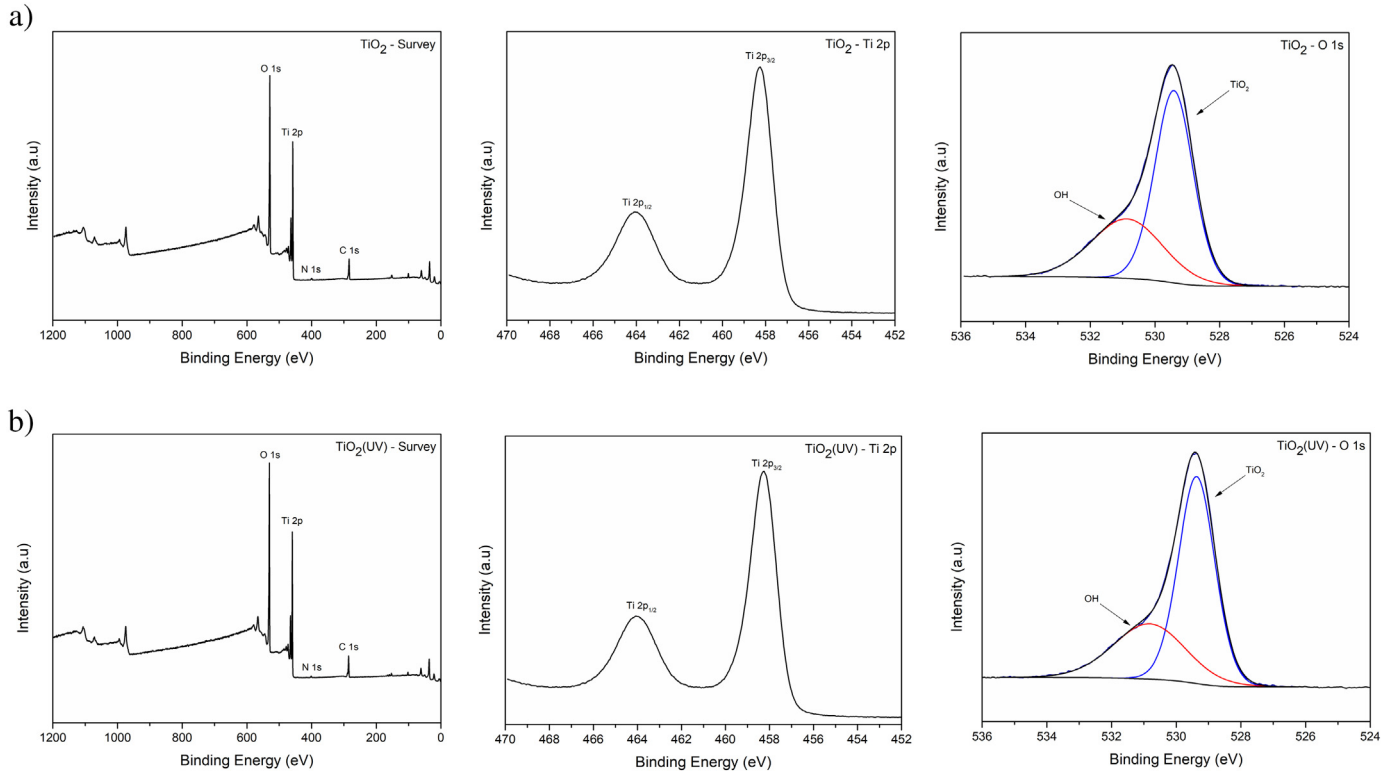

Fig. 2. (a) Survey and high resolution of O1s and Ti 2p XPS spectra for TiO_2 films and (b) Survey and high resolution of O 1s and Ti 2p XPS spectra for TiO_2 (UV) films.

45 min. However, other interfacial factors, as electrons in the surface, may interfere with the dispersive component, which would lead to a very similar surface energy between substrates exposed to different UV light times [89,90]. Therefore, it can be said that UV irradiation changes the chemical composition of nanoscale TiO_2 surface by modifying the electrostatic force on the oxide surface and its hydrophilicity. These changes act as the driving force for interaction between organic molecules and titania substrates. In general, the methods used for biofunctionalization of titanium metal surfaces, deposition and hydroxylation of TiO_2 promote a versatile film with polar characteristic from the bifunctional organic spacers, important in the implant/protein interface process.

To determine the physicochemical changes attributed to the TiO_2 photocatalytic phenomena, the titania surfaces, before (TiO_2) and after 45 min irradiation (TiO_2 (UV)), were characterized by X-ray photoelectron spectroscopy (XPS). The survey spectra contain Ti 2p (~460 eV), O 1s(~530 eV) and C 1s (~285 eV), but not other peaks (Fig. 2). The trace amount of carbon and nitrogen is likely due to the impurities of the substrate or adventitious contaminants. Both, TiO_2 and TiO_2 (UV) survey and high resolution Ti 2p and O1s XPS spectra, did not present significant differences. In this way it was not possible to evaluate modifications on the hydroxyl groups from TiO_2 (UV) surface.

Fig. 2 shows the high-resolution XPS spectra of Ti2p and O1s region of the TiO_2 surface. The 2p3/2 peaks of Ti and TiO_2 are known to be at 453.8 eV and 458.8 eV, respectively. The Ti2p spectrum revealed a clear Ti 2p3/2 peak at approximately e Ti 2p 1/2 peak, corresponding to the Ti(IV) of TiO_2. The energy difference between spin orbit peaks Ti $2p^1/_2$ and Ti $2p^3/_2$ is 5.7 eV which is consistent to Ti^{4+} in TiO_2 bond. The deconvolution the O1s peak shows two contributions that can be assigned to Ti—O in TiO_2 and —OH groups on the surface [91].

Binding energy and percentages of the Ti—O and —OH contributions were presented in Table 1. From Table 1 the hydroxyl groups contributions at the TiO_2 film surface, detected by XPS, are related to H_2O chemisorbed. [87,88] In fact, some studies [89] have already shown

Table 1
Positions and contributions of the Ti-O and -OH.

Surface	Binding energy (eV)	%
TiO_2	529.4 (Ti—O)	65.09
	530.9 (—OH)	34.91
TiO_2 (UV)	529.4 (Ti—O)	62.91
	530.8 (—OH)	36.18

that the decrease in surface hydroxyl groups was observed in XPS experiments when the measurement was maintained for 2–3 h after the introduction of the sample into the ultra-high vacuum (UHV) chamber from the equipment. This suggests that hydroxyl groups formed by UV irradiation can desorbed (desorption of surface water molecules) even at room temperature in the UHV chamber. Therefore, the detection of photocatalytic behavior does not occur through the spectroscopic technique, which in this case was performed after 12 h in the UHV chamber [90].

A number of studies involving the UV light treatment on the titania surface, confirm that increased hydrophilicity by decreasing the contact angle comes from a greater hydroxylation of the surface. The hydroxylation process is time reversible and the substrates must be immediately functionalized with the bifunctional compound of interest [91].

Titania substrates without irradiation (TiO_2) and irradiated for 45 min with UV lamp [TiO_2 (UV)] were immediately functionalized with the bisphosphonates alendronate and risedronate. Bisphosphonates tend to form self-assembled monolayers (SAMs) on the oxide surfaces of TiO_2 being able to form hydrolytically stable and strongly adhered to the substrates. Alendronate and risedronate have two functional groups, phosphate or amino, chemically capable of forming a covalent bond with hydroxyls groups present on the TiO_2 film surface, in order to obtain different chemical interfaces [40].

The main chemical element compositions of substrates were

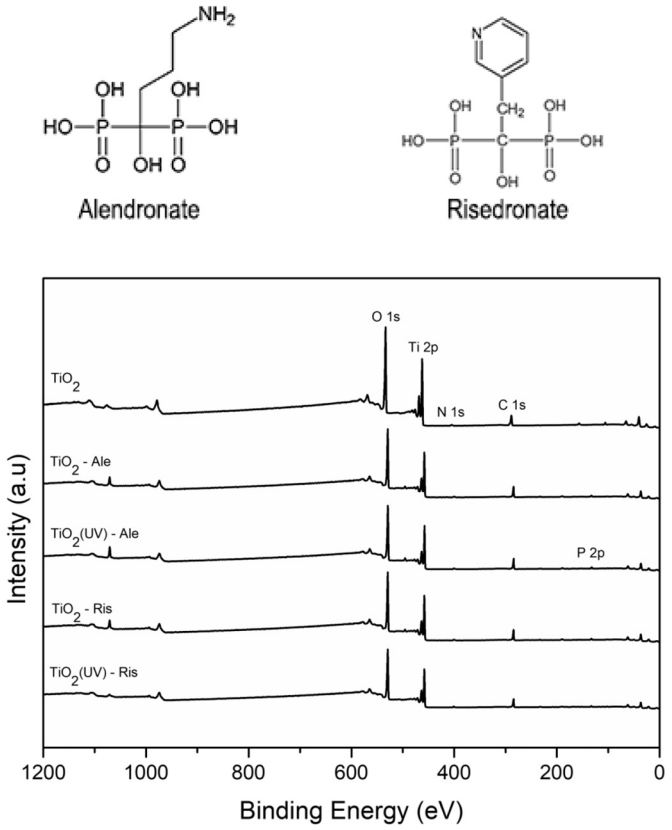

Fig. 3. Chemical structure of alendronate and risedronate and survey XPS spectra of TiO_2, TiO_2-Ale, TiO_2(UV)-Ale, TiO_2-Ris, and TiO_2(UV)-Ris.

observed by XPS. More information about the bisphosphonate chemical bond and the UV influence of hydroxylation substrate can be obtained from a careful analysis of high-resolution XPS scans. The bifunctional chemical compounds analyzed and the XPS survey spectra of TiO_2, TiO_2-Ale, TiO_2 (UV)-Ale, TiO_2-Ris and TiO_2 (UV)-Ris, are shown in Fig. 3.

Both survey spectra contain Ti 2p (~454 eV), O 1s (~530 eV), C1s (~285 eV), N 1s (~400 eV) and P 2p (~133 eV) signals confirming the adhesion of the bisphosphonates on the oxide surface. The N 1s and P 2p photoelectron signals are expected to be weak due to the lower quantity of these elements on the molecules structure. A peak at ~1072 eV is consequence of remaining Na from the functionalization process. All the samples showed a similar Ti 2p high-resolution spectrum when compared with the TiO_2 substrates, previously described.

Analyzing the O 1s, P 2p and N 1s high-resolution spectra (Fig. 4) for the functionalized samples it is possible to evaluate the mode of attachment of the bisphosphonates on the TiO_2 surface. Furthermore, these spectra allow evaluating the influence of UV treatment on the surface prior to functionalization. Most importantly, the P (2p) and N 1s signals confirm the presence of bisphosphonate adsorptions on the TiO_2 surface [72,92].

Analyzing the high-resolution N 1s, O 1s and P 2p spectra of alendronate on the TiO_2 and TiO_2 (UV) surface it is possible to understand a preferential binding mode on both substrates. The deconvolution of N 1s high-resolution spectrum for TiO_2-Ale shows that the main peak has two contributions centered at 396.4 eV and 399.7 eV, referent to Ti—N (or Ti—O—N) and a free C—NH_2/NH_2 from alendronate.

The TiO_2(UV)-Ale shows a N 1s peak with two contributions, centered at 398.5 and 400.7 eV, relative to free C—NH_2/NH_2 bonds [40,72,91,92].

The O 1s signal for TiO_2-Ale presents three contributions at 528.9 eV, 529.8 eV and 531.5 eV, which corresponds to TiO_2, Ti—O, and Ti—O—P/P═O bond, respectively. The same contributions were observed for TiO_2 (UV)-Ale, but centered at 529.1 eV, 530.1 eV and 531.5 eV. In this case, there is a reduction of the Ti—O contribution (about 13%) and a 5% increase on Ti—O—P/P═O contribution, which can be attributed to the higher number of hydroxyl groups on the TiO_2 (UV) surface [40,91]. The P 2p high resolution spectra deconvolution shown a characteristic asymmetric $P2p_{1/2}$ and $P2p_{3/2}$ for both substrates centered at 132.1 eV and 132.9 eV, confirming the presence of alendronate on the surface [91]. The TiO_2 (UV)-Ale presents alterations on the orbital electronic distribution with more electrons on the $P2p_{3/2}$, probably influenced by UV treatment on the TiO_2 surface.

The TiO_2-Ris and TiO_2 (UV)-Ris high resolution XPS spectra showed similar results with TiO_2-Ale and TiO_2 (UV)-Ale. The N1s spectrum of TiO_2-Ris presented tree contributions: the first at 396.4 eV is relative to Ti—N interaction; and the other two at higher energy at 401.0 eV and 398.9 eV are related to C═N/C—N bond. For TiO_2(UV)-Ris two N1s contributions were observed centered at 400.1 eV and 401.2 eV, related to C═N/C—N groups. The presence of these groups also indicates that the UV surface treatment directs the formation of specific binding between the bisphosphonates and the TiO_2 hydroxylated surface, leaving the C—N groups free on the surface. Oxygen 1s spectrum shows two peaks localized at 529.2 eV and 529.9 eV relative to TiO_2 and Ti—O bond. Another peak at 531.5 eV is also observed and can be assigned to the superposition between Ti—O—P and P═O bonds. The TiO_2(UV)-Ris presents identical contributions in 529.3 eV, 530.2 eV and 531.6 eV, with about 5% increase area variation. The P2p signals are similar to the asymmetric peaks obtained for substrates functionalized with alendronate. The 2p3/2 and 2p1/2 peaks appear centered on 132.3 eV and 133.7 eV, respectively for TiO_2-Ris. UV light treatment before functionalization also leads to an electronic redistribution in the $2p_{3/2}$ orbitals (132.9 eV) and $2p_{1/2}$ (133.7 eV) [92,93].

The information obtained by XPS is useful for understanding the configuration of the molecule on the surface. Fig. 5 shows possible modes of attachment for alendronate and risedronate molecules on the surface of titanium dioxide.

According to the analysis of the high-resolution N 1s, O 1s and P 2p spectra, TiO_2-Ale interacts with the surface according to models (a), (b) and (c) from Fig. 5. The TiO_2 (UV)-Ale has free NH_2 groups, binding through Ti—O—P interactions with the oxide surface, which may be mono-, bi- or tridentate. From XPS measurements it was not observed Ti—N bonds for TiO_2 (UV)-Ale samples, as observed in Fig. 5c. The substrate functionalized with risedronate shows the same behavior. For TiO_2-Ris three binding modes are possible, as can be seen in Fig. 5(d), (e) and (f). The UV light treatment also directs the mode of attachment for the TiO_2 (UV)-Ris on the oxide surface, and no Ti—N contributions are observed during the bisphosphonate immobilization. As reported by Zheng, et al., [72] the bisphosphonates interactions on hydroxylated surfaces involves the condensation between Ti—OH bond from the surface and P-OH groups from the bisphosphonates, forming mono-, bi-, or tridentate bonds. In addition, the P—OH and P═O groups present in alendronate immobilized on the TiO_2 (UV) surface may interact with an adjacent organic group or with hydroxyl or oxo groups on the substrate via hydrogen bonding [20,92–96]. Depending on the various possible bonding modes, it is difficult to predict the distribution of the chemical bonds and an exact surface structure [97]. The covalent bonding of the molecules on the surface is very important to understand the physicochemical properties of the surface, since they are determined by the final group on the surface.

As shown by XPS analysis the alendronate and risedronate surface properties are governed by amine groups and the pyridine ring, respectively. In addition, the use of surface treatment (UV radiation) directs the bonds on the surface of TiO_2 and homogeneous monolayers are obtained. The pendant end groups in the monolayer surface offer the reactions possibility with other organic groups of the interface, as proteins and cell, chemically modifying the surface and the cellular interaction [98–100].

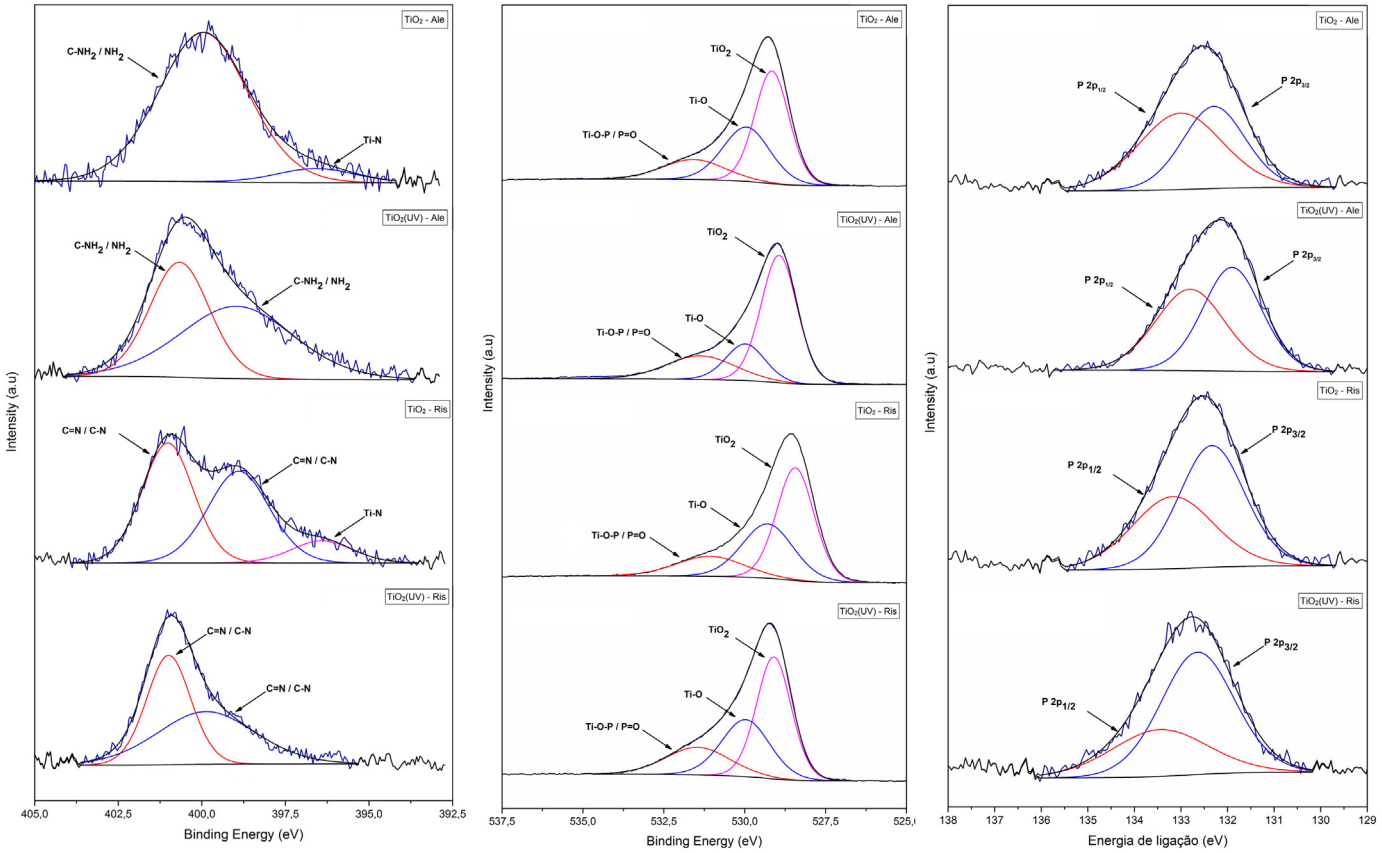

Fig. 4. High-resolution XPS spectra of N 1s, O 1s and P 2p for the functionalized samples.

As the chemical surface and topography alter the wettability of the surface, modulating the interactions that occur at the chemical interface from dental and orthopedic implants, water contact angle measurements and surface energy were performed for bisphosphonates functionalized substrates. The measurement was performed at 3 points for each sample in an ambient air, and the average value was used. The TiO_2(UV)-Ale and TiO_2 (UV)-Ris showed a contact angle of 9.9° and 21.3°, with surface energy of approximately 73.2 dyn/cm and 74.8 dyn/cm respectively, compared to the initial TiO_2(UV) contact angle (23.9°) and surface energy (72.41 dyn/cm). Fig. 6 shows the contact angle and surface energy values for the UV treated functionalized samples [101,102].

Generally, a hydrophobic surface has a contact angle > 90°, while a hydrophilic surface has a contact angle of < 90°. After alendronate functionalization of the TiO_2(UV) the surface became more hydrophilic with lower contact angle and consequently greater wettability. The TiO_2(UV)-Ris maintained the similar contact angle to TiO_2(UV). However, both TiO_2(UV)-Ale and TiO_2(UV)-Ris exhibited similar

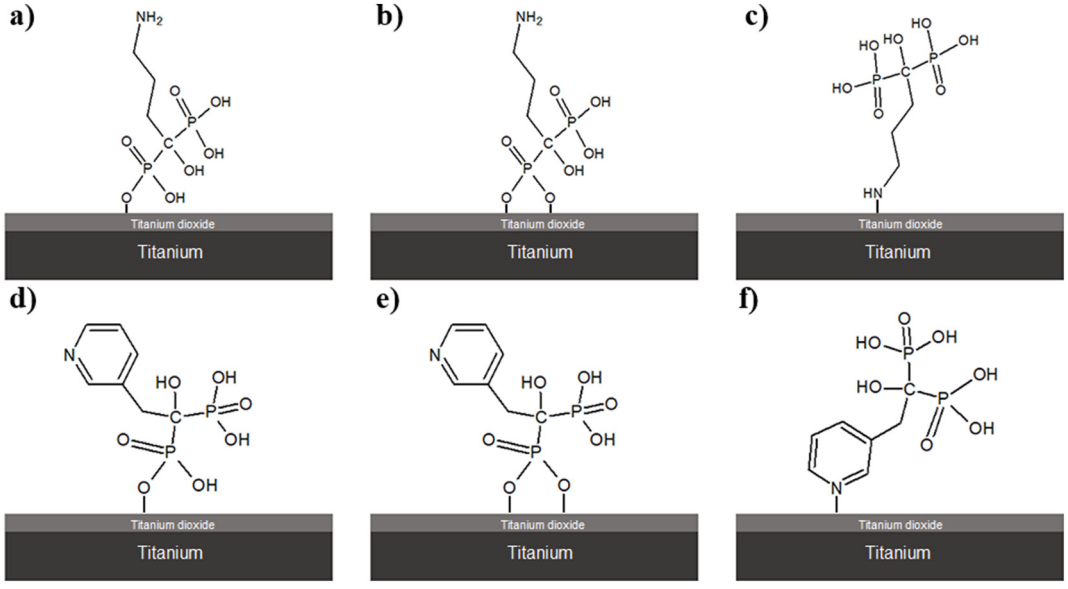

Fig. 5. Possible model of attachment upon TiO_2 surface for (a, b, c) alendronate and (d, e, f) risedronate.

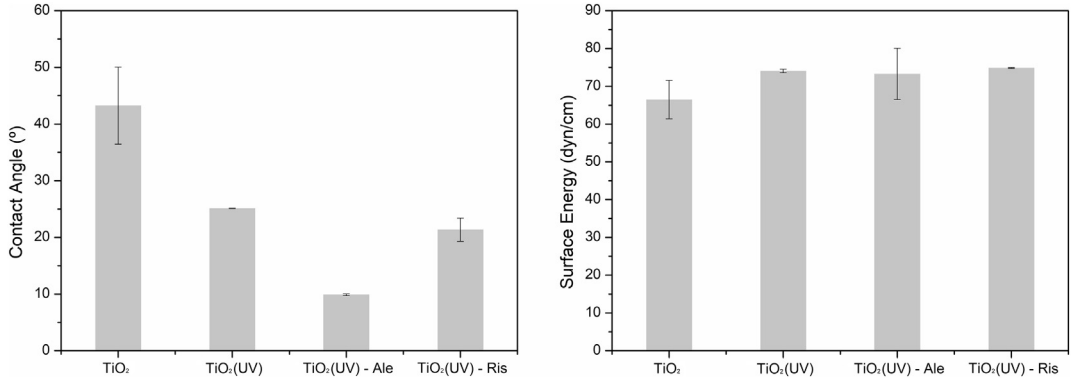

Fig. 6. Contact angle (a) and surface energy (b) measurements of TiO_2, TiO_2(UV), TiO_2(UV)-Ale and TiO_2(UV)-Ris substrates.

surface energy, due to contribution of different dispersive and polar components. In this case, the presence of hydroxyl and ionizable amino groups on the TiO_2(UV)-Ale surface contributed to the increase of the free-energy from the polar component with a reduction of the contact angle and consequently an increase in hydrophilicity. For TiO_2(UV)-Ris, beside the larger contact angle, it is believed that the pyridinium rings with electron resonance alter the polar and dispersive components, leading to a surface energy similar to that obtained for TiO_2(UV)-Ale. In view of this, both substrates have contact angles and free surface energy that confer hydrophilicity to the material favoring the proliferation of osteoblasts [103].

Topography and surface roughness were evaluated through AFM measurements. The results are presented in Fig. 7 and show the TiO_2(UV) and TiO_2(UV) functionalized films.

The results showed significant differences in TiO_2 surface after immobilization of the bisphosphonates. It can be observed that the oxide functionalization leads to increase the arithmetic surface nanoroughness (Ra) and became even more uniform after alendronate and risedronate functionalization [104].

The pre-osteoblast MC3T3-E1 cells cultured on titanium surfaces and modified substrates (TiO_2(UV), TiO_2(UV)-Ale and TiO_2(UV)-Ris were performed by the MTT reduction assay. MTT is a quantitative and commonly used method to evaluate the cellular response (viability/cytotoxicity) submitted to an external component, detecting increase or decrease of cells. Ti substrates were used as a control group because they are materials already used in implants with cytocompatibility and bioactivity evaluated [43,105,106].

The results of MTT optical density (OD) values at 570 nm are shown in Fig. 8. After 24 h of cell culture, it was possible to observe a great increase in the cellular viability for the functionalized substrates with alendronate and risedronate, even higher than TiO_2(UV) substrate. In 48 h of cell culture, a pronounced increase in cell viability for TiO_2(UV) substrates is observed when compared to TiO_2(UV)-Ale and TiO_2(UV)-Ris substrates. However, the TiO_2(UV)-Ale substrate shows a moderate increase between 24 and 48 h, while for TiO_2(UV)-Ris no significant differences were detected. After 72 h of cell culture, all the substrates presented reduction in the cell viability. Some studies associate this cellular viability reduction with advancement into the osteoblastic cell differentiation stages. The reciprocal relationship between decreased cell proliferation and induction of differentiation has been reported [107].

However, it is not possible to state from the biological tests carried out.

The influences of surface modifications treatment (UV radiation and bisphosphonate functionalization) showed to be significant for evaluation of the substrates as bone implants when compared metallic

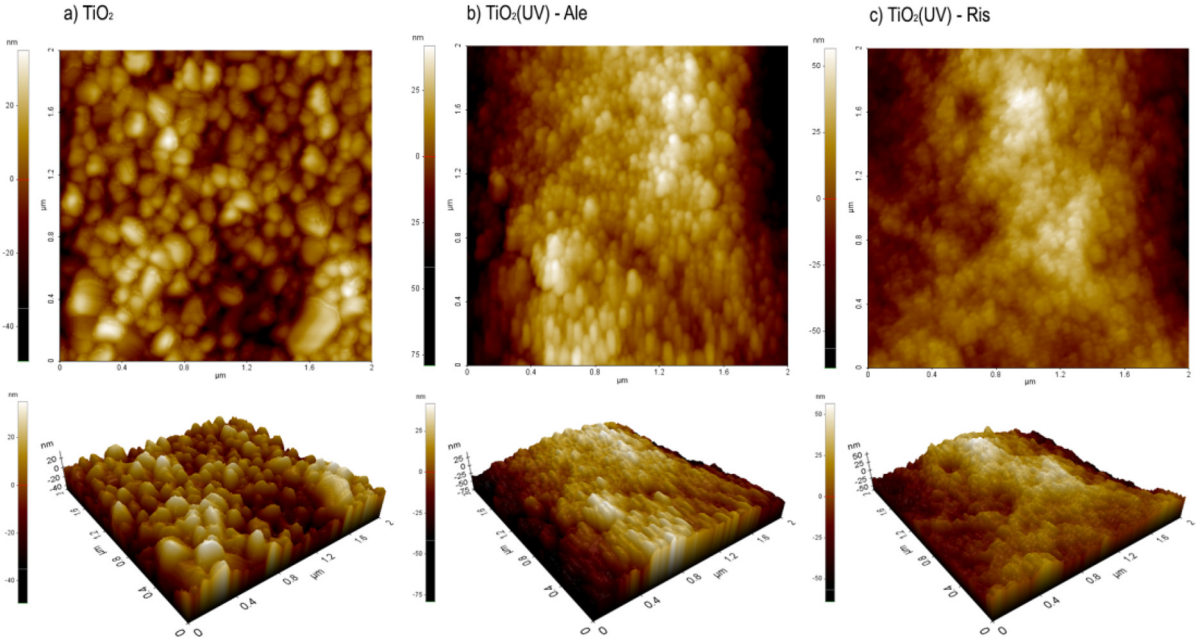

Fig. 7. Two-dimensional (on the top) and three-dimensional (down) AFM images of the surface of TiO_2 (R_a = 9.34 ± 0.2 nm) (a), TiO_2(UV)-Ale (R_a = 16.20 ± 0.77 nm) (b) and TiO_2(UV)-Ris (R_a = 16.55 ± 0.12 nm) (c).

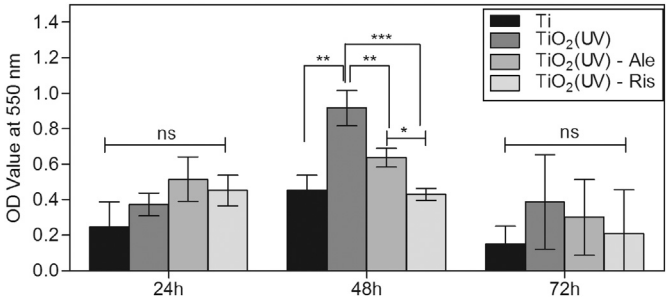

Fig. 8. Optical density (OD) measurements relative to MC3T3-E1 cell viability on Ti and TiO_2 substrates derivatives, after culturing for 24, 48 and 72 h (one-way ANOVA, black star, $p < 0.05$).

titanium. In general, the functionalization of the surface alters the physicochemical properties of the surface and even so, it is favorable for adhesion and proliferation of osteoblasts.

SEM observation (Fig. 9) after 48 h of cell culture showed that pre-osteoblasts morphology adhered on surfaces. Both surfaces have adequate adhesion and proliferation to MC3T3-E1 cells as assessed in the cell viability results. The cells have a rounded and/or ovoid morphology with cytoplasmatic extensions. The adherent cells displayed a rounded or polygonal polarized shape on functionalized surfaces.

Calcium deposition (mineralization) is one of the most significant indications for bone formation and the differentiation of osteoblasts is one of the key processes. The in vitro MC3T3-E1 differentiation into osteoblast was qualitatively obtained by Alizarin Red staining assay. In this procedure, extracellular matrix mineralization (ECM), the areas of calcification in the cells, are stained in red by Alizarin Red staining through the specific calcium binding sites.

The representative image of calcified matrix deposition at 14 days is shown in Fig. 10.

It can be noticed a slight reddish coloration and formation of a layer on the surface of the substrates (Ti, TiO_2(UV) and TiO_2(UV)-Ris) with evidence of formation of mineralized nodules and with evident accumulation of collagen. The TiO_2(UV)-Ale substrate showed no evidence of mineralization after 14 days.

The cell can be stimulated basically for two distinct situations: proliferation or differentiation/synthesis. In the case of pre-osteoblasts there may be a stimulus for proliferation, with increased cell viability results, however without mineralization. On the other hand, when stimulated for differentiation (induction with beta glycerophosphate and ascorbic acid after 2 days of adhesion) in osteoblasts and bone production (or in vitro mineralization nodules), these cells will stop proliferating. Therefore the results of cell viability may be lower in this case, since the cells have not proliferated but differentiated in blasts. In summary, the results may suggest that cells on the surface of TiO_2 (UV)-Ale proliferated rather but did not differentiate into osteoblasts.

Studies have shown that the initial collagen production can be altered by topography and surface hydrophilicity [107, 108]. It is known that in osteogenic medium, MC3T3-E1 cells follow a developmental process, including an initiation phase (1–2 week), in which cells proliferate slowly, express ALP activity and other bone specific genes, resulting in the formation of collagen matrix. During the second maturation phase (2–4 weeks) the mineralized matrix formation is observed. The mineralization nodules are considered, in vitro, a functional point that reflects cell differentiation [63].

In this context, the topography of the implant surface affects the cellular behavior, the rate and extension of the interfacial bone formation, altering the biomechanical quality of the newly formed and the adherent extracellular matrix formation and mineralization. Thus, the presence of bisphosphonates structures on the TiO_2 surface tends to alter the time formation of mineralized matrix, altering the production of fundamental collagen in the properties of osseointegration, influencing the physical properties of the extracellular matrix [63].

4. Conclusions

This study demonstrates the chemical and physical effects on TiO_2-

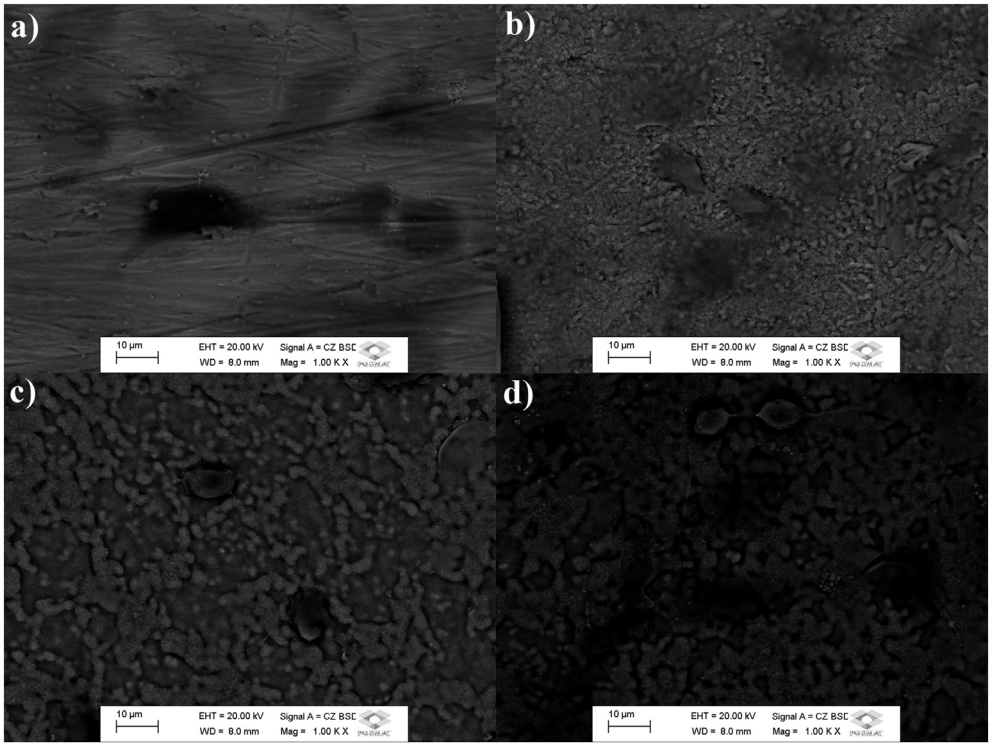

Fig. 9. Scanning electron microscopy (SEM) of MC3T3-E1 cells cultured after 48 h on (a) Ti, (b) TiO_2(UV), (c) TiO_2(UV)-Ale and (d) TiO_2(UV)-Ris substrates derivatives at ×1000 magnification.

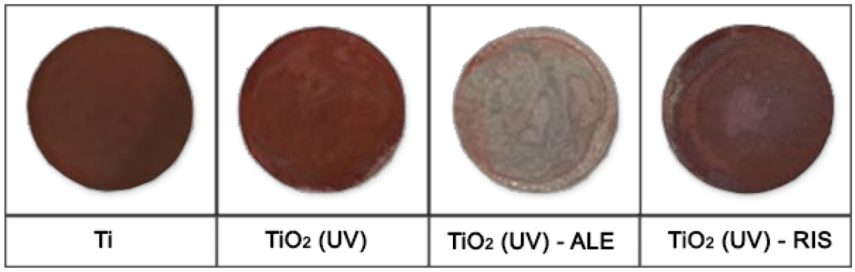

Fig. 10. Alizarin Red staining of MC3T3-E1 osteoblasts. The cells were cultured at 14 on (a) Ti, (b) TiO_2(UV), (c) TiO_2(UV)-Ale and (d) TiO_2(UV)-Ris. (For interpretation of the references to color in this figure legend, the reader is referred to the web version of this article.)

coated Ti cp4 surfaces, by UV treatment and functionalization with bisphosphonates, specifically alendronate and risedronate. The TiO_2 film deposited on Ti cp4 by spin coating technique presents a chemically hydroxylated surface that allows the covalent attachment with bifunctional compounds. The work has shown that the UV light treatment of surfaces changes the chemical properties, like wettability. Furthermore, the UV treatment allowed an orderly and oriented immobilization of alendronate and risedronate on the TiO_2 film surface, forming monolayers. TiO_2 (UV) sample presented greater cell viability in 48 h, the behavior of the functionalized groups showed better viability when compared to the Ti control, normally used in biological implants.

In addition, the functionalized surface with bisphosphonates also exhibit the hydrophilicity required in literature, TiO_2 (UV)-Ale and TiO_2 (UV)-Ris have a contact angle of 9.9° and 21.3°, suitable for viability and mineralization of pre-osteoblastic cells. However, the surface chemistry played a significant role in cell mineralization, since TiO_2(UV)-Ale with $-NH_2$ groups on surface showed low potential for calcium formation in 14 days, even with high cell adhesion and viability. Therefore, these compounds emerge as a potential treatment on implants surfaces.

Acknowledgment

The authors thank FAPESP grants (2014/01713-3, 2014/20471-0, 2016/11183-7 and 2017/15035-5) and CAPES, for financial support. They are also grateful to Dra. Bruna Carolina Costa of São Paulo State University (UNESP), Bauru, Brazil for the SEM images, Professor Elidiane C. Rangel of São Paulo State University (UNESP), Institute of Science and Technology, Sorocaba, Brazil for the contact angle and energy surface measurements and Heloisa Helenna Figueiredo Paes de Oliveira for image design.

References

[1] T. Hanawa, A comprehensive review of techniques for biofunctionalization of titanium, J Periodontal Implant Sci. 41 (2011) 263–272.
[2] V.P. Mantripragada, B. Lecka-Czernik, N.A. Ebraheim, A.C. Jayasuriya, An overview of recent advances in designing orthopedic and craniofacial implants, J. Biomed. Mater. Res. A 101 (2013) 3349–3364.
[3] M. Niinomi, M. Nakai, J. Hieda, Development of new metallic alloys for biomedical applications, Acta Biomater. 8 (2012) 3888–3903.
[4] M. Geetha, A.K. Singh, R. Asokamani, A.K. Gogia, Ti based biomaterials, the ultimate choice for orthopaedic implants – a review, Prog. Mater. Sci. 54 (2009) 397–425.
[5] X. Liu, S. Chen, J.K.H. Tsoi, J.P. Matinlinna, Binary titanium alloys as dental implant materials—a review, Regenerative Biomaterials (2017) 315–323.
[6] M. Abdel-Hady Gepreel, M. Niinomi, Biocompatibility of Ti-alloys for long-term implantation, J. Mech. Behav. Biomed. Mater. 20 (2013) 407–415.
[7] I. Wall, N. Donos, K. Carlqvist, F. Jones, P. Brett, Modified titanium surfaces promote accelerated osteogenic differentiation of mesenchymal stromal cells in vitro, Bone 45 (2009) 17–26.
[8] R.A. Gittens, R. Olivares-Nvarrete, A. Cheng, D.M. Anderson, T. McLachlan, I. Stephan, J. Geis-Gerstorfer, K.H. Sandhage, A.G. Fedorov, F. Rupp, B.D. Boyan, R. Tannenbaum, Z. Schwartz, The roles of titanium surface micro/nanotopography and wettability on the differential response of human osteoblast lineage cells, Acta Biomater. 9 (2013) 6268–6277.
[9] L.D. Trino, L.F.G. Dias, L.G.S. Albano, E.S. Bronze-Uhle, E.C. Rangel, C.F.O. Graeff, P.N. Lisboa-Filho, Zinc oxide surface functionalization and related effects on corrosion resistance of titanium implants, Ceram. Int. 44 (2018) 4000–4008.
[10] A. Ochsenbeina, F. Chai, S. Winter, M. Traisnel, J. Breme, H.F. Hildebrand, Osteoblast responses to different oxide coatings produced by the sol–gel process on titanium substrates, Acta Biomater. 4 (2008) 1506–1517.
[11] M.F. Maitz, U. Freudenberg, M.V. Tsurkan, M. Fischer, T. Beyrich, C. Werner, Bioresponsive polymer hydrogels homeostatically regulate blood coagulation, Nat. Commun. 4 (2013).
[12] Y. Sul, B. Kang, C. Johansson, H. Um, C. Park, T. Albrektsson, The roles of surface chemistry and topography in the strength and rate of osseointegration of titanium implants in bone, J. Biomed. Mater. Res. A 89 (2009) 942–950.
[13] J.S. Shah, P.K.C. Venkatsurya, W.W. Thein-Han, R.D.K. Misra, T.C. Pesacreta, M.C. Somani, L.P. Karjalainen, The role of nanocrystalline titania coating on nanostructured austenitic stainless steel in enhancing osteoblasts functions for regeneration of tissue, Mater. Sci. Eng. C 31 (2011) 458–471.
[14] X. Chen, S.S. Mao, Titanium dioxide nanomaterials: synthesis, properties, modifications, and applications, Chem. Rev. 107 (2007) 2891–2959.
[15] V. Zorba, X. Chen, S.S. Mao, Superhydrophilic TiO_2 surface without photocatalytic activation, Appl. Phys. Lett. 96 (2016) 093702.
[16] H. Chen, S. Huang, T. Perng, Highly transparent hard bio-coating synthesized by low temperature sol–gel process, Surf. Coat. Technol. 233 (2013) 140–146.
[17] P. Silva-Bermudez, S.E. Rodil, An overview of protein adsorption on metal oxide coatings for biomedical implants, Surf. Coat. Technol. 233 (2013) 147–158.
[18] D.P. Macwan, P.N. Dave, A review on nano-TiO_2 sol-gel type syntheses and its applications, J. Mater. Sci. 46 (2011) 3669–3686.
[19] F. Rupp, M. Haupt, H. Klostermann, H. Kim, M. Eichler, A. Peetsch, L. Scheideler, C. Doering, C. Oehr, H.P. Wendel, S. Sinn, E. Decker, C. Ohle, J. Geis-Gerstorfer, Multifunctional nature of UV-irradiated nanocrystalline anatase thin films for biomedical applications, Acta Biomater. 6 (2010) 4566–4577.
[20] O. Pop-Georgievski, D. Kubies, J. Zemek, N. Neykova, R. Demianchuk, E.M. Chánová, M. Šlouf, M. Houska, F. Rypáček, Self-assembled anchor layers/polysaccharide coatings on titanium surfaces: a study of functionalization and stability, Beilstein J. Nanotechnol. 6 (2015) 617–631.
[21] J.C. Love, L.A. Estroff, J.K. Kriebel, R.G. Nuzzo, G.M. Whitesides, Self-assembled monolayers of thiolates on metals as a form of nanotechnology, Chem. Rev. 105 (2005) 1103–1169.
[22] J.Y. Lim, J.C. Hansen, C.A. Siedlecki, J. Runt, H.J. Donahue, Human foetal osteoblastic cell response to polymer-demixed nanotopographic interfaces, J. R. Soc. Interface 2 (2005) 97–108.
[23] C.A. Scotchford, C.P. Gilmore, E. Cooper, G.J. Leggett, S. Downes, Protein adsorption and human osteoblast-like cell attachment and growth on alkylthiol on gold self-assembled monolayers, J. Biomed. Mater. Res. 59 (2002) 84–99.
[24] T. Hanawa, A comprehensive review of techniques for biofunctionalization of titanium, J. Periodontal Implant Sci. 41 (2011) 263–272.
[25] M.E. Simonsen, Z. Li, E.G. Søgaard, Influence of the OH groups on the photocatalytic activity and photoinduced hydrophilicity of microwave assisted sol–gel TiO_2 film, Appl. Surf. Sci. 255 (2009) 8054–8062.
[26] M. Nakamura, L. Sirghi, T. Aoki, Y. Hatanaka, Study on hydrophilic property of hydro-oxygenated amorphous TiO_x:OH thin films, Surf. Sci. 507 (2002) 778–782.
[27] M. Miyauchi, N. Kieda, S. Hishita, T. Mitsuhashi, A. Nakajima, T. Watanabe, K. Hashimoto, Reversible wettability control of TiO_2 surface by light irradiation, Surf. Sci. 511 (2002) 401–407.
[28] X.-P. Wang, Y. Yu, X.-F. Hu, L. Gao, Hydrophilicity of TiO_2 films prepared by liquid phase deposition, Thin Solid Films 371 (2000) 148–152.
[29] R. Wang, K. Hashimoto, A. Fujishima, M. Chikuni, E. Kojima, A. Kitamura, M. Shimohigoshi, T. Watanabe, Light-induced amphiphilic surfaces, Nature 388 (1997) 431–432.
[30] S. Choi, W. Jeong, J. Cha, J. Lee, K. Lee, H. Yu, E. Choi, K. Kim, C. Hwang, Overcoming the biological aging of titanium using a wet storage method after ultraviolet treatment, Sci. Rep. 7 (2017) 3833–3844.
[31] M. Takeuchi, K. Sakamoto, G. Martra, S. Coluccia, M. Anpo, Mechanism of photoinduced superhydrophilicity on the TiO_2 photocatalyst surface, J. Phys. Chem. B 109 (2005) 15422–15428.
[32] R. Wang, K. Hashimoto, A. Fujishima, M. Chikuni, E. Kojima, A. Kitamura, M. Shimohigoshi, T. Watanabe, Light-induced amphiphilic surfaces, Nature 388 (1997) 431–432.
[33] K. Yadav, B.R. Mehta, K.V. Lakshmi, S. Bhattacharya, J.P. Singh, Tuning the

wettability of indium oxide nanowires from Superhydrophobic to nearly superhydrophilic: effect of oxygen-related defects, J. Phys. Chem. C 119 (2015) 16026–16032.
[34] J.C. Yu, J. Yu, W. Ho, J. Zhao, Light-induced super-hydrophilicity and photocatalytic activity of mesoporous TiO_2 thin films, J. Photochem. Photobiol., A 148 (2002) 331–339.
[35] M.S.A. Qahtani, Y. Wu, S. Spintzyk, P. Krieg, A. Killinger, E. Schweizer, I. Stephan, L. Scheideler, J. Geis-Gerstorfer, F. Rupp, UV-A and UV-C light induced hydrophilization of dental implants, Dent. Mater. 31 (2015) 157–167.
[36] L. Li, S. Kim, S. Cho, Comparison of alkaline phosphatase activity of MC3T3-E1 cells cultured on different Ti surfaces: modified sandblasted with large grit and acid-etched (MSLA), laser-treated, and laser and acid-treated Ti surfaces, J. Adv. Prosthodont. 8 (2016) 235–240.
[37] C.C. Wachesk, C.A.F. Pires, B.C. Ramos, V.J. Trava-Airoldi, A.O. Lobo, C. Pacheco-Soares, F.R. Marciano, N.S. Da-Silva, Cell viability and adhesion on diamond-like carbon films containing titanium dioxide nanoparticles, Appl. Surf. Sci. 266 (2013) 176–181.
[38] J.W. Park, J.H. Jang, C.S. Lee, T. Hanawa, Osteoconductivity of hydrophilic microstructured titanium implants with phosphate ion chemistry, Acta Biomater. 5 (2009) 2311–2321.
[39] Y. Huang, X. Zhang, R. Zhao, H. Mao, Y. Yan, X. Pang, Antibacterial efficacy, corrosion resistance, and cytotoxicity studies of copper-substituted carbonated hydroxyapatite coating on titanium substrate, J. Mater. Sci. 50 (2015) 1688–1700.
[40] N. Metoki, L. Liu, E. Beilis, N. Eliaz, D. Mandler, Preparation and characterization of alkylphosphonic acid self-assembled monolayers on titanium alloy by chemisorption and electrochemical deposition, Langmuir 30 (2014) 6791–6799.
[41] N. Adden, L.J. Gamble, D.G. Castner, A. Hoffmann, G. Gross, H. Menzel, Phosphonic acid monolayers for binding of bioactive molecules to titanium surfaces, Langmuir 22 (2006) 8197–8204.
[42] E.S. Gawalt, M.J. Avaltron, M.P. Danahy, B.M. Silverman, E.L. Hanson, K.S. Midwood, J.E. Schwarzbauer, J. Schwartz, Bonding organics to Ti alloys: facilitating human osteoblast attachment and spreading on surgical implant materials, Langmuir 19 (2003) 200–204.
[43] S. Bozzini, P. Petrini, M.C. Tanzi, S. Zürcher, S. Tosatti, Poly(ethylene glycol) and hydroxy functionalized alkane phosphate mixed self-assembled monolayers to control nonspecific adsorption of proteins on titanium oxide surfaces, Langmuir 26 (2010) 6529–6534.
[44] F. Knocha, C. Jaquieryb, M. Kowalskya, S. Schaeren, C. Alabrea, I. Martinb, H.E. Rubasha, A.S. Shanbhaga, Effects of bisphosphonates on proliferation and osteoblast differentiation of human bone marrow stromal cells, Biomaterials 26 (2005) 6941–6949.
[45] H.G. Bone, D. Hosking, J.O. Devogelaer, J.R. Tucci, R.D. Emkey, R.P. Tonino, J.A. Rodriguez-Portales, R.W. Downs, J. Gupta, A.C. Santora, U. Liberman, Ten years' experience with alendronate for osteoporosis in postmenopausal women, N. Engl. J. Med. 350 (2004) 1189–1199.
[46] J.P. Walsh, L.C. Ward, G.O. Stewart, R.K. Will, R.A. Criddle, R.L. Prince, B.G. Stuckey, S.S. Dhaliwal, C.I. Bhagat, R.W. Retallack, G.N. Kent, P.J. Drury, S. Vasikaran, D.H. Gutteridge, A randomized clinical trial comparing oral alendronate and intravenous pamidronate for the treatment of Paget's disease of bone, Bone 34 (2004) 747–754.
[47] M.J. Rogers, J.C. Frith, S.P. Luckman, F.P. Coxon, H.L. Benford, J. Monkkonen, S. Auriola, K.M. Chilton, G.G. Russell, Molecular mechanisms of action of bisphosphonates, Bone (1999) 24.
[48] M. Yoshinari, Y. Oda, H. Ueki, S. Yokose, Immobilization of bisphosphonates on surface modified titanium, Biomaterials 22 (2001) 709–715.
[49] B.M. Bell, R.E. Bell, Oral bisphosphonates and dental implants: a retrospective study, Int. J. Oral Maxillofac. Surg. 66 (2008) 1022–1024.
[50] S.E. Papapoulos, Bisphosphonate actions: physical chemistry revisited, Bone 38 (2006) 613–616.
[51] R.G.G. Russell, P.I. Croucher, J.M. Rogers, Bisphosphonates: pharmacology, mechanisms of action and clinical uses, Osteoporos. Int. 2 (1999) 66–80.
[52] A.J. Roelofs, C.A. Stewart, S. Sun, K.M. Blazewska, B.A. Kashemirov, C.E. McKenna, R.G.G. Russel, M.J. Rogers, M.W. Lundy, F.H. Ebetino, F.P. Coxon, Influence of bone affinity on the skeletal distribution of fluorescently labeled bisphosphonates in vivo, J. Bone Miner. Res. 27 (2012) 835–847.
[53] G.H. Nancollas, R. Tang, R.J. Phipps, Z. Henneman, S. Gulde, W. Wu, A. Mangood, R.G.G. Russell, F.H. Ebetino, Novel insights into actions of bisphosphonates on bone: differences in interactions with hydroxyapatite, Bone 38 (2006) 617–627.
[54] M.J. Rogers, J.C. Crockett, F.P. Coxon, J. Mönkkönen, Biochemical and molecular mechanisms of action of bisphosphonates, Bone 49 (2011) 34–41.
[55] Y. Gao, S. Zou, X. Liu, C. Bao, J. Hu, The effect of surface immobilized bisphosphonates on the fixation of hydroxyapatite-coated titanium implants in ovariectomized rats, Biomaterials 30 (2009) 1790–1796.
[56] J. Grischke, J. Eberhard, M. Stiesch, Antimicrobial dental implant functionalization strategies —a systematic review, Dent. Mater. J. 35 (2016) 545–558.
[57] T. Bellido, L.I. Plotkin, Novel actions of bisphosphonates in bone: preservation of osteoblast and osteocyte viability, Bone 49 (2011) 50–55.
[58] L.D. Trino, E.S. Bronze-Uhle, A. George, M.T. Mathew, P.N. Lisboa-Filho, Surface physicochemical and structural analysis of functionalized titanium dioxide films, Colloids Surf. A Physicochem. Eng. Asp. 546 (2018) 168–178.
[59] M. Lewandowska, A. Rogusk, M. Pisarek, B. Polak, M. Janik-Czachor, K.J. Kurzydłowski, Morphology and chemical characterization of Ti surfaces modified for biomedical application, Biomol. Eng. 24 (2007) 438–444.
[60] J.F. Moulder, Handbook of X-ray Photoelectron Spectroscopy, Perkin-Elmer Corporation, Minnesota, 1992.
[61] D.K. Owens, R.C. Wendt, Estimation of the surface free energy of polymers, J. Appl. Polym. Sci. 13 (1969) 1741–1747.
[62] C.C. Wachesk, C.A.F. Pires, B.C. Ramos, V.J. Trava-Airoldi, A.O. Lobo, C. Pacheco-Soares, F.R. Marciano, N.S. Da-Silva, Cell viability and adhesion on diamond-like carbon films containing titanium dioxide nanoparticles, Appl. Surf. Sci. 266 (2013) 176–181.
[63] K. Subramani, S.N. Pandruvada, D.A. Puleo, J.K. Hartsfield, S.S. Huja, In vitro evaluation of osteoblast responses to carbon nanotube-coated titanium surfaces, Prog. Orthod. 17 (23) (2016).
[64] T. Mosmann, Rapid colorimetric assay for cellular growth and survival: application to proliferation and cytotoxicity assays, J. Immunol. Methods 65 (1983) 55–63.
[65] F.A. Oliveira, A.A. Matos, S.S. Matsuda, M.A. Buzalaf, V.S. Bagnato, M.A. Machado, et al., Low level laser therapy modulates viability, alkaline phosphatase and matrix metalloproteinase-2 activities of osteoblasts, J. Photochem. Photobiol. B 28 (2017) 35–40.
[66] M.P. Silva, A.A. Matos, J.V. Paulin, R.A.S. Alavarce, R.C. Oliveira, C.F.O. Graeff, Biocompatibility investigations of synthetic melanin and melanin analogue for application in bioelectronics, Polym. Int. 65 (2016) 1347–1354.
[67] D. Lattner, H.P. Jennissen, Preparation and properties of ultra-hydrophilic surfaces on titanium and steel, Materialwiss. Werkstofftech. 40 (2009) 108–116.
[68] F. Rupp, L. Scheideler, N. Olshanska, M. Wild, M. Wieland, J. Geis-Gerstorfer, Enhancing surface free energy and hydrophilicity through chemical modification of microstructured titanium implant surfaces, J. Biomed. Mater. Res. A 76 (2006) 323–334.
[69] F.A. Oliveira, A.A. Matos, M.R. Santesso, C.K. Tokuhara, A.L. Leite, V.S. Bagnato, et al., Low intensity lasers differently induce primary human osteoblast proliferation and differentiation, J. Photochem. Photobiol. B 163 (2016) 14–21.
[70] C. Legrand, J.M. Bour, C. Jacob, J. Capiaumont, A. Martial, A. Marc, M. Wudtke, G. Kretzmer, C. Demangel, D. Duval, J. Hache, Lactate dehydrogenase (LDH) activity of the number of dead cells in the medium of cultured eukaryotic cells as marker, J. Biotechnol. 25 (1992) 231–243.
[71] B. Tian, S. Tang, Y. Li, T. Long, X.Qu.D. Yu, Y. Guo, P. Guo, Z. Zhu, Fabrication, characterization, and biocompatibility of ethyl cellulose/carbonated hydroxyapatite composite coatings on Ti6Al4V, J. Mater. Sci. Mater. Med. 25 (2014) 2059–2068.
[72] D. Zheng, K.G. Neoh, E. Kang, Immobilization of alendronate on titanium via its different functional groups and the subsequent effects on cell functions, J. Colloid Interface Sci. 487 (2017) 1–11.
[73] P. van der Valk, A.W.J. van Pelt, H.J. Busscher, H.P. Jong, C.R.H. Wildevuur, J. Arends, Interaction of fibroblasts and polymer surfaces: relationship between surface free energy and fibroblast spreading, J. Biomed. Mater. Res. 17 (1983) 807–817.
[74] P. van Wachem, A.H. Hogt, T. Beugeling, J. Feijen, A. Bantjes, J.P. Detmers, W.G. van Aken, Adhesion of cultured human endothelial cells onto methacrylate polymers with varying surface wettability and charge, Biomaterials 8 (1987) 323–328.
[75] C. Vasilescu, P. Drob, E. Vasilescu, I. Demetrescu, D. Ionita, M. Prodana, S.I. Drob, Characterization and corrosion resistance of the electrodeposited hydroxyapatite and bovine serum albumin/hydroxyapatite films on Ti–6Al–4V–1Zr alloy surface, Corros. Sci. 53 (2011) 992–999.
[76] H. Aita, N. Hori, M. Takeuchi, T. Suzuki, M. Yamada, M. Anpo, T. Ogawa, The effect of ultraviolet functionalization of titanium on integration with bone, Biomaterials 30 (2009) 1015–1025.
[77] R.A. Gittens, L. Scheideler, F. Rupp, S.L. Hyzy, J. Geis-Gerstorfer, Z. Schwartz, B.D. Boyan, A review on the wettability of dental implant surfaces II: biological and clinical aspects, Acta Biomater. 10 (2014) 2907–2918.
[78] J.H. Park, C.E. Wasilewski, N. Almodovar, R. Olivares-Navarrete, B.D. Boyan, R. Tannenbaum, Z. Schwartz, The responses to surface wettability gradients induced by chitosan nanofilms on microtextured titanium mediated by specific integrin receptors, Biomaterials 33 (2012) 7386–7393.
[79] K. Law, H. Zhao, Surface Wetting: Characterization, Contact Angle, and Fundamentals, Springer, New York, 2016.
[80] A.W. Adamson, A.P. Gast, Physical Chemistry of Surfaces, six edition, Wiley-Interscience Publication, New York, 1997.
[81] K.M. Hotchkiss, G.B. Reddy, S.L. Hyzy, Z. Schwartz, B.D. Boyan, R. Olivares-Navarrete, Titanium surface characteristics, including topography and wettability, alter macrophage activation, Acta Biomater. 31 (2016) 425–434.
[82] M.E. Marques, A.A.P. Mansur, H.S. Mansur, Chemical functionalization of surfaces for building three-dimensional engineered biosensors, Appl. Surf. Sci. 275 (2013) 347–360.
[83] K. Yadav, B.R. Mehta, K.V. Lakshmi, S. Bhattacharya, J.P. Singh, Tuning the wettability of indium oxide nanowires from Superhydrophobic to nearly superhydrophilic: effect of oxygen-related defects, J. Phys. Chem. C 119 (2015) 16026–16032.
[84] R. Sun, A. Nakajima, A. Fujishima, T. Watanabe, K. Hashimoto, Photoinduced surface wettability conversion of ZnO and TiO_2 thin films, J. Phys. Chem. B 105 (2001) 1984–1990.
[85] I. Jang, K. Song, J.H. Park, S.G. Oh, Enhancement of dye adsorption on TiO_2 surface through hydroxylation process for dye-sensitized solar cells, Bull. Kor. Chem. Soc. 34 (2013) 2883–2888.
[86] W. Toshiya, Y. Naoya, Wettability control of a solid surface by utilizing photocatalysis, Chem. Rec. 8 (2008) 279–290.
[87] J.C. Yu, J.G. Yu, W.K. Ho, J.C. Zhao, Light-induced superhydrophilicity and photocatalytic activity of mesoporous TiO2 thin films, J. Photochem. Photobiol., A 148 (2002) 331–339.
[88] F. Rupp, M. Haupt, H. Klostermann, H. Kim, M. Eichler, A. Peetsch, L. Scheideler,

C. Doering, C. Oehr, H.P. Wendel, S. Sinn, E. Decker, C. von Ohle, J. Geis-Gerstorfer, Multifunctional nature of UV-irradiated nanocrystalline anatase thin films for biomedical applications, Acta Biomater. 6 (2010) 4566–4577.
[89] N. Sakai, A. Fujishima, T. Watanabe, K. Hashimoto, Quantitative evaluation of the photoinduced hydrophilic conversion properties of TiO_2 thin film surfaces by the reciprocal of contact angle, J. Phys. Chem. B 107 (2003) 1028–1035.
[90] T. Zubkov, D. Stahl, T.L. Thompson, D. Panayotov, O. Diwald, J.T. Yates, Ultraviolet light-induced hydrophilicity effect on $TiO_2(110)(1\times1)$. Dominant role of the photooxidation of adsorbed hydrocarbons causing wetting by water droplets, J. Phys. Chem. B 109 (2005) 15454–15462.
[91] L. Rojo, B. Gharibi, R. McLister, B.J. Meenan, S. Deb, Self-assembled monolayers of alendronate on Ti6Al4V alloy surfaces enhance osteogenesis in mesenchymal stem cells, Sci. Rep. 6 (2016) 30548–30558.
[92] K. McLeod, S. Kumar, R.St.C. Smart, N. Dutta, N.H. Voelcker, G.I. Anderson, R. Sekel, XPS and bioactivity study of the bisphosphonate pamidronate adsorbed onto plasma sprayed hydroxyapatite coatings, Appl. Surf. Sci. 253 (2006) 2644–2651.
[93] K. Rudzka, A.Y.S. Trevino, M.A. Rodríguez-Valverde, M.A. Cabrerizo-Vílchez, Formation of mixed and patterned self-assembled films of alkylphosphonates on commercially pure titanium surfaces, Appl. Surf. Sci. 389 (2016) 270–277.
[94] G. Guerrero, P.H. Mutin, A. Vioux, Anchoring of phosphonate and phosphinate coupling molecules on titania particles, J. Mater. Chem. 13 (2001) 4367–4373.
[95] A. Ide, G.L. Drisko, N. Scales, V. Luca, C.H. Schiesser, R.A. Caruso, Monitoring bisphosphonate surface functionalization and acid stability of hierarchically porous titanium zirconium oxides, Langmuir 27 (2011) 12985–12995.
[96] F. Brodard-Severac, G. Guerrero, J. Maquet, P. Florian, C. Gervais, P.H. Mutin, High-field 17O MAS NMR investigation of phosphonic acid monolayers on titania, Chem. Mater. 20 (2008) 5191–5196.
[97] Y. Paz, Self-assembled monolayers and titanium dioxide: from surface patterning to potential applications, Beilstein J. Nanotechnol. 2 (2011) 845–861.
[98] G. Tan, L. Zhang, C. Ning, X. Liu, J. Liao, Preparation and characterization of APTES films on modification titanium by SAMs, Thin Solid Films 519 (2011) 4997–5001.
[99] J. Zuo, E. Torres, Comparison of adsorption of Mercaptopropyltrimethoxysilane on amphiphilic TiO_2 and hydroxylated SiO_2, Langmuir 26 (2010) 15161–15168.
[100] H. Schweikl, R. Muller, C. Englert, K.A. Hiller, R. Kujat, M. Nerlich, G. Schmalz, Proliferation of osteoblasts and fibroblasts on model surfaces of varying roughness and surface chemistry, J. Mater. Sci. Mater. Med. 18 (2007) 1895–1905.
[101] L. Feller, Y. Jadwat, R.A.G. Khammissa, R. Meyerov, I. Schechter, J. Lemmer, Cellular responses evoked by different surface characteristics of intraosseous titanium implants, Biomed. Res. Int. 2015 (2015).
[102] Z.H. Zheng, L. Zhang, L.J. Kong, A.J. Wang, Y.D. Gong, X.F. Zhang, The behavior of MC3T3-E1 cells on chitosan/poly-L-lysine composite films: effect of nanotopography, surface chemistry, and wettability, J. Biomed. Mater. Res., Part A 89A (2008) 453–465.
[103] B. Tian, S. Tang, Y. Li, T. Long, X. Qu, D. Yu, Fabrication, characterization, and biocompatibility of ethyl cellulose/carbonated hydroxyapatite composite coatings on Ti6Al4V, J. Mater. Sci. Mater. Med. 25 (2014) 2059–2068.
[104] E.S. Gawalt, M.J. Avaltroni, N. Koch, J. Schawartz, Self-assembly and bonding of alkanephosphonic acids on the native oxide surface of titanium, Langmuir 17 (2001) 5736–5738.
[105] W. Wang, T.L. Li, H.M. Wong, P.K. Chu, R.Y.T. Kao, S. Wu, F.K.L. Leung, T.M. Wong, M.K.T. To, K.M.C. Cheung, K.W.K. Yeung, Development of novel implants with self-antibacterial performance through in-situ growth of 1D ZnO nanowire, Colloids Surf., B 141 (2016) 623–633.
[106] Y. Huang, X. Zhang, R. Zhao, H. Mao, Y. Yan, X. Pang, Antibacterial efficacy, corrosion resistance, and cytotoxicity studies of copper-substituted carbonated hydroxyapatite coating on titanium substrate, J. Mater. Sci. 50 (2015) 1688–1700.
[107] E.S. Thian, Z. Ahmad, J. Huang, M.J. Edirisinghe, S.N. Jayasinghe, D.C. Ireland, R.A. Brooks, N. Rushton, W. Bonfield, S.M. Best, The role of surface wettability and surface charge of electrosprayed nanoapatites on the behaviour of osteoblasts, Acta Biomater. 6 (2010) 750–755.
[108] D.B.S. Mendonça, P.A. Miguez, G. Mendonça, M. Yamauchi, F.J.L. Aragão, L.F. Cooper, Titanium surface topography affects collagen biosynthesis of adherent cells, Bone 49 (2011) 463–472.